Aging effects and dynamic scaling in the 3D Edwards-Anderson spin glasses: a comparison with experiments

M. Picco[1], F. Ricci-Tersenghi[2,a], and F. Ritort[3]

[1] LPTHE, Université Pierre et Marie Curie - Paris VI, Université Denis Diderot - Paris VII, Boite 126, Tour 16, 1er étage, 4 place Jussieu, 75252 Paris Cedex 05, France

[2] Abdus Salam International Center for Theoretical Physics, Condensed Matter Group, Strada Costiera 11, PO Box 586, 34100 Trieste, Italy

[3] Department of Physics, Faculty of Physics, University of Barcelona, Diagonal 647, 08028 Barcelona, Spain

Abstract. We present a detailed study of the scaling behavior of correlations functions and AC susceptibility relaxations in the aging regime in three-dimensional spin glasses. The agreement between simulations and experiments is excellent confirming the validity of the full aging scenario with weak sub-aging effects.

PACS. 75.10.Nr Spin-glass and other random models – 75.40.Gb Dynamic properties (dynamic susceptibility, spin waves, spin diffusion, dynamic scaling, etc.) – 75.40.Mg Numerical simulation studies

1 Introduction

There is a great interest in the understanding of dynamical effects in spin glasses. These include magnetization relaxation, aging and temperature change protocols [1–5]. The study of these effects may clarify the nature of spatial effects and coarsening phenomena in spin glasses, an issue which remains still poorly understood.

In this paper we present a detailed study of magnetization relaxation phenomena and aging effects in three-dimensional Edwards-Anderson spin glasses. Our primary goal is to check the validity of the full $t/t_{\rm w}$ scaling behavior in correlation functions as well as identifying possible sources of corrections to that behavior by comparing to experimental data. Dynamical experiments in spin glasses include magnetic relaxation and AC measurements. Here we will focus our attention on correlation function and AC susceptibility relaxations. The advantage of studying correlations is that these are easy to evaluate numerically being also tightly related to thermoremanent magnetization relaxation experiments. On the other hand, AC relaxations can be directly compared to experimental results and, to the best of our knowledge, no results appeared on this point in the literature.

There exist many works on simulations in the literature [6–9] studying correlations or remanent magnetization relaxations and this part of the topic that we investigate here is certainly not new. What has never been considered in detail in the past and merits further investigation is the explicit comparison between simulations and experiments. Having the experimental results in mind we

[a] e-mail: `riccife@ictp.trieste.it`

have tried to apply the same scaling plots used by the experimentalists to our numerical data. This may serve as a valuable guide to better understand what properties are generic to spin glasses and what coarsening scenario accounts for the collected experimental data.

Magnetic relaxation (or correlation function) and AC experiments give equivalent information, the advantage of using AC experiments is that they constitute a very sensitive tool to detect dissipative processes. When measuring correlations the external time scale $t_{\rm w}$ is fixed by the time elapsed after quenching below $T_{\rm c}$ while in AC experiments the external time scale is fixed by the inverse of the frequency of the AC field. In a full scaling scenario, in the first class of experiments the relevant scaling variable is $t/t_{\rm w}$ while in the second class it is ωt. In what follows we check the validity of this simple scaling behavior identifying possible sources of corrections.

2 The model and the observables

The Edwards-Anderson model [10] is defined by the following Hamiltonian

$$\mathcal{H} = -\sum_{(i,j)} J_{ij}\sigma_i\sigma_j - h\sum_{i=1}^{V}\sigma_i, \qquad (1)$$

where the indices i, j run from 1 to V, the σ_i are Ising spins ($\sigma_i = \pm 1$) and the pairs (i, j) identify nearest neighbors in a three-dimensional lattice. The exchange couplings J_{ij} are taken from a random distribution. The simplest choice

is a Gaussian distribution with zero average and finite variance,

$$\mathcal{P}(J) = \left(\frac{1}{2\pi}\right)^{\frac{1}{2}} \exp\left(-\frac{J^2}{2}\right). \qquad (2)$$

This model displays a spin glass transition at finite temperature $T_c \simeq 0.95$ [11,12]. A Monte Carlo step corresponds to a sweep over V randomly chosen spins of the lattice. Monte Carlo simulations of (1) use random updating of the spins with the Metropolis algorithm. Dynamical experiments use very large lattices (typical sizes are in the range $L = 20$–100) with negligible finite-size effects for the largest sizes ($L = 64$ for magnetization relaxation experiments and $L = 100$ for AC experiments). Correlation function simulations have been done on a special purpose machine APE100 [13] for sizes 64^3 and averaged over 10 samples. AC experiments were done for a single sample on a Linux cluster of PC's for size $L = 100$.

Relaxation measurements are done applying a uniform magnetic field and measuring the decay of the thermoremanent magnetization (hereafter denoted by TRM), or equivalently, the growth of the zero-field cooled (ZFC) magnetization. The typical experiment consists in the following. A sample is fast quenched below the spin glass transition temperature and let to relax for a waiting time t_w. Then a uniform small magnetic field h is applied and the growth of the magnetization measured,

$$\chi_{ZFC}(t_w, t_w + t) = \frac{1}{Vh} \sum_{i=1}^{V} \sigma_i(t_w + t). \qquad (3)$$

Another quantity of interest related to the magnetization which can be numerically investigated is the two-time correlation defined by

$$C(t_w, t_w + t) = \frac{1}{V} \sum_{i=1}^{V} \sigma_i(t_w)\sigma_i(t_w + t). \qquad (4)$$

The interest of studying correlations instead of zero-field cooled magnetizations is that they yield the same dynamical information. Indeed in the stationary regime they are related through the fluctuation-dissipation theorem (FDT)

$$\chi_{ZFC}(t) = \frac{1 - C(t)}{T}. \qquad (5)$$

In AC experiments an oscillating magnetic field $h(t) = h_0 \cos(2\pi\omega t)$ of frequency $\omega = \frac{1}{P}$, where P is the period, is applied to the system and the magnetization measured as a function of time

$$M(t) = M_0 \cos(2\pi\omega t + \phi), \qquad (6)$$

where M_0 is the intensity of the magnetization and ϕ is the dephasing between the magnetization and the field. The origin of the dephasing is dissipation in the system which prevents the magnetization to follow the oscillations of the magnetic field. From the magnetization one can obtain the in-phase and out-of-phase susceptibilities defined as

$$\chi' = \frac{M_0 \cos(\phi)}{h_0} = \frac{2\int_0^P M(t)\cos(2\pi\omega t)\mathrm{d}t}{h_0}, \qquad (7)$$

$$\chi'' = \frac{M_0 \sin(\phi)}{h_0} = \frac{2\int_0^P M(t)\sin(2\pi\omega t)\mathrm{d}t}{h_0}. \qquad (8)$$

The dephasing ϕ measures the rate of dissipation in the system and is given by

$$\tan(\phi) = \frac{\chi''}{\chi'}. \qquad (9)$$

In numerical simulations the in-phase and out-of-phase susceptibilities are computed by averaging the right-hand side in equations (7, 8) over several periods $P = \frac{1}{\omega}$. This means a very large measurement time for low frequencies for both experiments and simulations.

In the numerical simulations (both in DC or AC experiments) the intensity of the probing fields cannot be arbitrarily small because of the weakness of the signal in comparison to other source of fluctuations such as finite-size effects (which induce finite-volume statistical fluctuations for extensive quantities, like the susceptibility). Consequently, the intensities of the probing magnetic fields used in numerical simulations are much larger than the corresponding experimental ones (between 50 and 500 times larger). As we will comment later, we do not believe that this leads to conflicting results between simulations and experiments. As soon as one checks that measurements are done within the linear response regime then the intensity of the probing field should not be crucial. Actually the values of the intensity of the fields usually employed in numerical simulations of TRM experiments are well known to satisfy linear response [14,15]. Note that, in general, similar difficulties are encountered when analyzing data in both numerical simulations and real experiments, the main difference is the absolute magnitude of the time scales one can explore in the two cases (up to microseconds in simulations and between seconds and days in experiments).

3 TRM and correlation function relaxations

In order to study time scaling in a wide times range (specially in the aging $t \gg t_w$ regime) experimentalists have measured the decay of the TRM [3], which is strictly related to the zero-field-cooled one through $M_{ZFC} = M_{FC} - M_{TRM}$, where the field-cooled magnetization is practically constant in the glassy phase.

From the numerical simulations point of view the best quantity one can look at for checking time scaling is the autocorrelation function $C(t_w, t_w + t)$. It has much less fluctuations than any response to an external field. Moreover in the quasi-equilibrium regime where the fluctuation-dissipation theorem (FDT) holds, it gives exact information on the zero-field-cooled susceptibility *via*

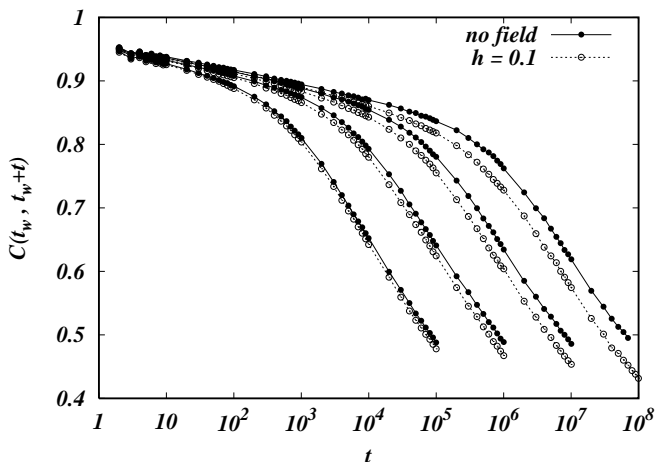$$\chi(t_w, t_w + t) = \frac{1 - C(t_w, t_w + t)}{T}. \qquad (10)$$

Fig. 1. Aging at $T = 0.5$ with and without an external magnetic field after time t_{w} for a 64^3 system. Waiting times (t_{w}) range from 10^3 (leftmost curves) to 10^6 (rightmost curves).

In the aging regime the connection between correlation and susceptibility is less trivial. However in the limit of small perturbing field and large times, where a generalization of the FDT seems to hold [15–17], a relation between correlation and susceptibility can still be established. Then, in general, concerning time scaling, we can safely assume that the autocorrelation functions decay as the TRM do.

In this section we try to understand which is the best scaling for the $C(t_{\mathrm{w}}, t_{\mathrm{w}} + t)$ data. The measurements have been taken on 10 samples of a 64^3 system, at a temperature $T = 0.5$, with waiting times ranging up to $t_{\mathrm{w}} = 10^6$ and measuring times up to $t = 10^8$. We have considered two different experimental situations, that is with or without an external magnetic field after time t_{w} (the evolution up to time t_{w} being always with no field), in order to check whether such a small perturbation may change the dynamical scaling. The external field intensity $h = 0.1$ has been chosen such that the system is in the linear response regime. If the magnetic field would be applied during all the experiment we do not expect any sensible difference with the $h = 0$ case.

In Figure 1 we show the correlation functions data, with and without the external magnetic field. As the time goes on the effect of the magnetic field seems to accumulate and the differences become larger. Note however that, for any given waiting time t_{w}, the correlation curve presents the two well known regimes [7,18]: the quasi-equilibrium one ($t < t_{\mathrm{w}}$) and the aging one ($t > t_{\mathrm{w}}$).

Because we are mainly interested in the scaling in the aging regime, we have tried, as the simplest analysis, to collapse the $t > t_{\mathrm{w}}$ data using t/t_{w}^μ as the scaling variable. The results are shown in Figure 2 and they clearly show that a value for μ smaller than 1 is needed in order to collapse the data in the large times limit. Note also that the presence of an external field seems to decrease sensibly the value of μ. The errors on the estimation of μ are of the order of 10^{-2}.
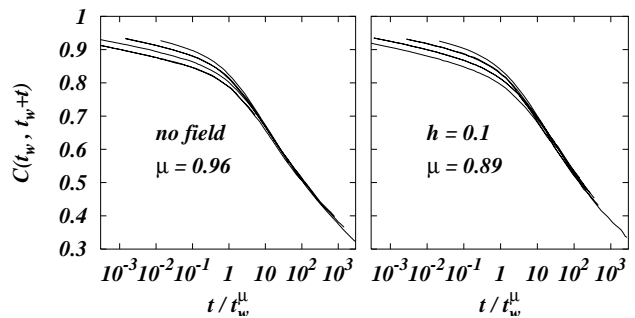

Fig. 2. Best scaling in the aging regime ($t > t_{\mathrm{w}}$) for the data presented in Figure 1.
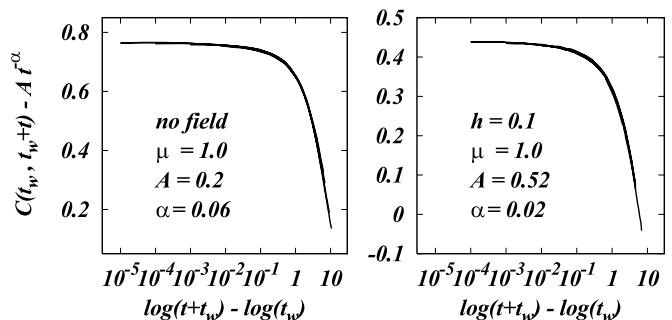

Fig. 3. Full aging ($\mu = 1$) data collapse for the correlations functions presented in Figure 1. Note that the use of a logarithmic scale improves the quality of data collapsing.

This numerical result may suggest the presence of a sub-aging regime in the EA model [19] and it could be interpreted as one more similarity with real spin glasses, where $\mu = 0.97$ [3]. However a more careful analysis shows that the correlation functions are perfectly compatible with a full aging, that is t/t_{w}, scaling. In Figure 3 we present the results of such an analysis, which has been done following the one performed on experimental TRM data in reference [3].

Few comments are in order. Assuming for the correlation $C(t_{\mathrm{w}}, t_{\mathrm{w}} + t)$ the scaling

$$C(t_{\mathrm{w}}, t_{\mathrm{w}} + t) = A \left(\frac{t_0}{t} \right)^\alpha + \hat{C}(t/t_{\mathrm{w}}), \qquad (11)$$

with $t_0 = 1$, then the best values for the A and α parameters seem to be similar to the experimental ones ($A = 0.1$ and $\alpha = 0.02$). However, because of the lack of a quantitative criterion for data collapsing, the best collapse is very often subjective. In this case we have found that, in order to obtain a good data collapse, the μ parameter must be fixed to 1 or very close to it. On the other hand, the A and α parameters are strongly correlated (with a correlation coefficient close to -1) and they can be changed by a quite large amount without affecting the data collapse. Then the errors on these parameters are large. In Figure 3 we show the collapse for parameters values being more or less in the center of the confidence region. We have also tried to collapse both sets of data ($h = 0$ and $h = 0.1$)

with the same parameters, but it was impossible to obtain any reasonable data collapse.

Let us note *en passant* that the strong dependence of the parameter A on the field is maybe due to a partial re-initialization induced by the field. Indeed in the numerical experiment where a small field in switched on at time t_{w} we are actually measuring the correlation between the configuration recorder at time t_{w} in the absence of any field and the one at time t which is feeling an external field. These configurations may partially differ because of the strong re-initialization effects produced by the application of an external magnetic field [24].

In Figure 3 we use the scaling variable $\log(t + t_{\mathrm{w}}) - \log(t_{\mathrm{w}})$, even if t/t_{w} would be the most natural one when full aging holds. Our choice is dictated by the need for a comparison with the collapse of experimental data shown in Figure 3b of reference [3]. There the scaling variable $[(t + t_{\mathrm{w}})^{1-\mu} - t_{\mathrm{w}}^{1-\mu}]/(1 - \mu)$ is used, which tends to $\log(t + t_{\mathrm{w}}) - \log(t_{\mathrm{w}})$ in the $\mu \to 1$ limit. It is well known that the goodness of a data collapse may depend on the scales chosen for presenting the data. In the present case, in the scaling variable $\log(t + t_{\mathrm{w}}) - \log(t_{\mathrm{w}})$ we have better collapses that in the variable t/t_{w}, because large times are "compressed". Note however that both scaling variables give very good collapses of our data, the same being true for the experimental data [20]. Anyhow it is worth to note that the use of the scaling variable t/t_{w} for checking full aging and $[(t+t_{\mathrm{w}})^{1-\mu}-t_{\mathrm{w}}^{1-\mu}]/(1-\mu)$ for checking sub-aging makes the life harder to the full aging scenario. This without considering the fact that there could be additional logarithmic corrections to the full t/t_{w} scaling [19].

We conclude that it is not easy to obtain precise quantitative information in order to distinguish the full aging from the sub-aging scenario. Moreover the presence of an external magnetic field, which on a first simple analysis seems to change the scaling, is in fact irrelevant for the scaling and it only changes a little bit the fitting parameters.

3.1 A small note on the ZFC susceptibility scaling

The scaling of the zero-field cooled susceptibility has been already studied in the past, both directly [7] or *via* the fluctuation-dissipation relation which links it to the correlation functions scaling [17]. Here we do not repeat this kind of analysis. We simply would like to present some new data regarding the ZFC susceptibility scaling.

Indeed very recently Bernardi *et al.* have proposed the following scaling for the ZFC susceptibility [21]

$$\chi_{\mathrm{ZFC}}(t_{\mathrm{w}}, t_{\mathrm{w}} + t) = \tilde{\chi}(R(t_{\mathrm{w}}), L(t)), \qquad (12)$$

where both length scales grow in an algebraic fashion

$$R(\tau) \propto L(\tau) \propto \tau^{aT}, \qquad (13)$$

with an exponent linear in the temperature, like for the off-equilibrium correlation length [8,9,22]. We found that numerical data obtained with very large simulations are not compatible with the proposed scaling (see Fig. 4).
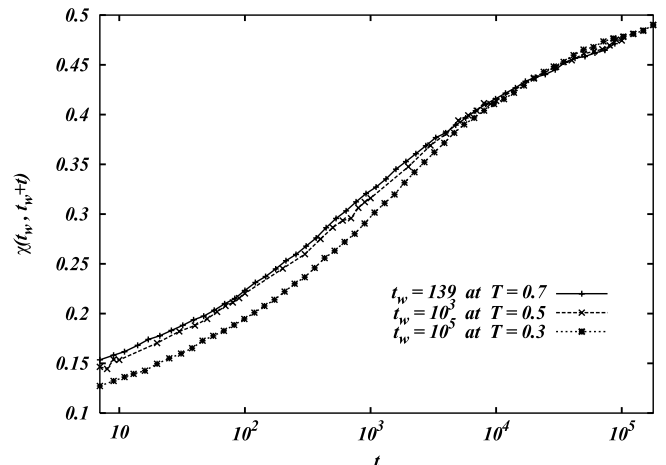

Fig. 4. ZFC susceptibilities in a particular experiment (see text). If the scaling (12) proposed in reference [21] would be correct, data in the figure should collapse.

Our numerical experiments are performed in the following way. For any given temperature T_1 (which takes 3 values in our case $T_1 = 0.3, 0.5, 0.7$), we start the simulation from a random configuration and we let evolve the system at temperature T_1 for a number of MCS t_{w}, such that $t_{\mathrm{w}}^{T_1} = D$ where D is a constant that we fixed to $D = 10^{1.5}$. At this time we switch on a small perturbing field, we move the temperature to $T_2 = 0.5$ and then we measure the response of the system (ZFC susceptibility). From this kind of experiment we have obtained many interesting information on the spin glass low temperature dynamics which have been published elsewhere [24]. Here we used again this kind of experiment in order to verify the scaling (12) proposed in reference [21].

By construction we have that in all the three experiments the length $R(t_{\mathrm{w}})$ is the same and the $L(t)$ is related to t by the same law, because after time t_{w} we always make evolve the system at the same temperature. Then if the scaling (12) would hold, we should find a good data collapse in Figire 4, which is not true. This behavior can be explained by observing that after the thermalization time $t_{\mathrm{w}}(T_1)$ the three experimental situations are not identical: they have developed a similar correlation length, nevertheless the actual configuration is different and the response to an external perturbation differs.

In reference [21] the authors find a perfect agreement to the scaling (12). However it must be noted that they use temperatures in a small range, $T \in [0.5, 0.7]$, which corresponds to the two uppermost curves in Figure 4 which indeed almost coincide. Violation to the scaling (12) can be seen only at lower temperatures, which where not used in reference [21].

4 AC susceptibility relaxations

Let us briefly remind how these experiments are usually done. The system is quenched to a low temperature (ranging between 0.6 and 0.9 times the value of T_g) and the AC
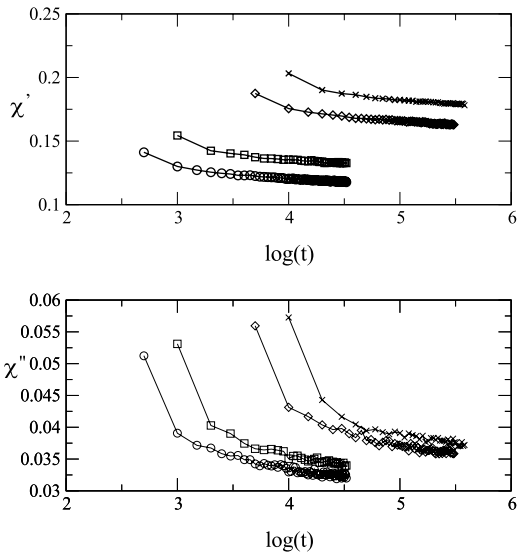
Fig. 5. AC susceptibility for $L = 100, T = 0.6$ and frequencies $\omega = 1/P = 0.02$ (circles), 0.01 (squares), 0.002 (diamonds), 0.001 (crosses).

Table 1. Fit parameters for the decay of the out-of-phase susceptibility. Data have been fitted starting from $\omega t = 30$ up to the end of available data.

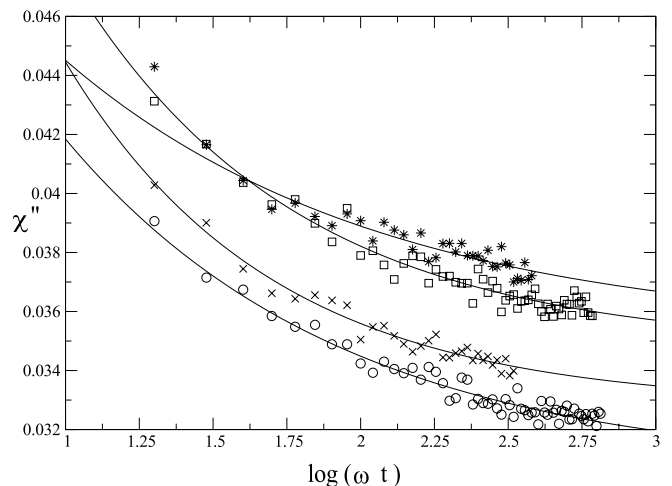| ω	$\chi''(\omega, \infty)$	B	x
0.02	0.031(1)	0.033(6)	0.46(7)
0.01	0.033(1)	0.050(10)	0.61(10)
0.002	0.034(1)	0.047(10)	0.57(10)
0.001	0.035(1)	0.023(10)	0.41(10)

Fig. 6. AC susceptibility for $L = 100, T = 0.6$ and frequencies $\omega = 1/P = 0.02, 0.01, 0.002, 0.001$ plotted as a function of ωt together with the best fits obtained from Table 1.

susceptibility is recorded. Typical values of the frequency of the AC field are between 0.1 and 1 Hertz. The amplitude of the probing AC field is of order 10^{-2} to 10^{-1} Oersteds deep inside the linear response regime. The AC susceptibility is then recorded as a function of time and relaxation is observed on time scales of order $\omega t \sim 1000-5000$ corresponding to several thousands of periods of the AC field. Measurements are then obtained averaging over several cycles of the AC field in order to obtain χ' and χ'' with enough accuracy (10 cycles is a typical value).

Having in mind the experimental setup we have done the following experiment. Starting from a random configuration we have measured the AC susceptibility as a function of time for different frequencies of the AC magnetic field. The frequencies of the field are defined as $\omega = \frac{1}{P}$ where P is the period of the oscillating field in Monte Carlo steps. The results for the *in-phase* and *out-of-phase* susceptibilities are shown in Figure 5 at temperature $T = 0.6 \simeq 0.63 T_c$ and field periods $P = 50, 100, 500, 1000$. Each point in equations (7) and (8) is obtained by averaging over 10 periods of the field. The curves for χ can be well fitted to power law decays. The biggest signal is obtained for the dissipative part χ'' which can be fitted to, $\chi''(\omega, t) = \chi''(\omega, \infty) + B (\omega t)^{-(1-x)}$ where the parameters x and B are expected to be frequency independent if the scaling t/t_w holds. In Table 1 we show the best fit parameters and we note two facts:

1. Within errors, B and x are essentially ω independent justifying the validity of the ωt scaling. B is around 0.04 and x is around 0.5 but with a big uncertainty. More statistics is necessary to determine better the fitting parameters. Unfortunately, going to large values of ωt for the smallest ω is computationally prohibitive.

2. $\chi''(\omega, \infty)$ seems to systematically increase when ω decreases. This result is unexpected. We would rather expect that $\chi''(\omega, \infty) \sim \omega^{\alpha}$ with $\alpha \simeq 0.06$ (according to Fig. 3). There are two possibilities to explain this discrepancy. First, α is so small that the correct dependence of $\chi''(\omega, \infty)$ on ω is masked by the other parameters of the fit. Second, frequencies are too big to see the asymptotic ω^{α} behavior. This second possibility would suggest that frequencies are not still in the asymptotic low-frequency regime and this could be related to the discrepancy between the simulation results in [24] and the real experimental results. Actually, comparison with the stationary results obtained for χ under slow cooling suggest indeed that χ'' is decreasing with the frequency for the range of frequencies explored. More refined statistics is necessary to resolve this question.

To make evident the ωt scaling for the AC experiment we show in Figures 6 and 7 the results of Figure 5 plotted *vs.* ωt. In Figure 6 these are plotted together with the power laws obtained with the fitting parameters of Table 1. In Figure 7 the values of the susceptibilities in the vertical scale have been shifted by an arbitrary quantity to make them coincide. This last procedure is exactly the same as done in experiments in the Figure 2 of reference [3] showing the same qualitatively results. Note from
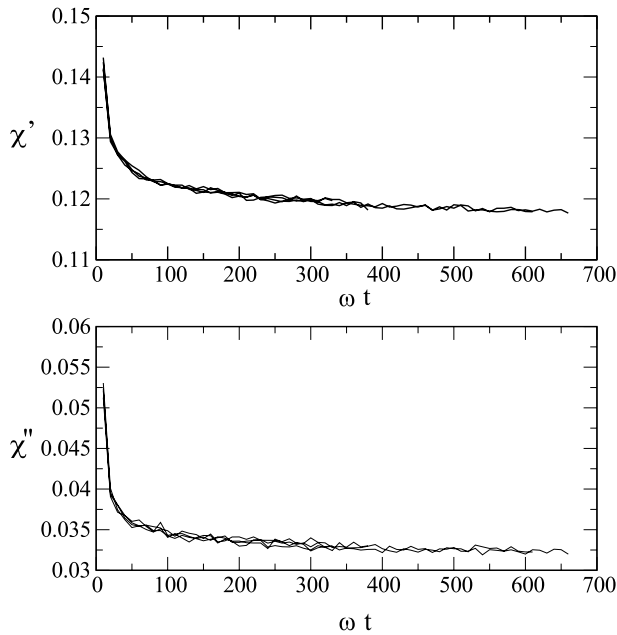
Fig. 7. Same data as in Figures 5, 6. Following reference [3] susceptibilities have been shifted on the vertical scale by arbitrary amounts to make them collapse.

Anderson model. A similar conclusion is obtained also for AC experiments which, in general, fulfill a good ωt scaling law. The collapse of the AC relaxations on a master curve, by appropriately shifting them by their stationary values shows a nice agreement with experimental results and shows how relaxation in disordered systems are described (at least in a very good approximation) by a single timescale (corresponding to the waiting time in TRM experiments or to the inverse of the frequency in AC experiments).

Still, the big question must be answered. Why this good agreement between simulations and experiments is not respected when comparing, at a qualitative level, chaotic and memory effects between the Edwards-Anderson model and real spin glasses? [23–25]. It is plausible that for time scales short compared to experimental time scales some dynamical effects (in particular, chaos and memory) are not seen in simulations while the full $t/t_{\rm w}$ scaling is already present in this regime. This would be a possible explanation if the observed anomalous behavior of $\chi''(\omega, \infty)$ (*i.e.* the fact that it increases when the frequency decreases) is a consequence of the shortness of the timescales involved in the simulation. Further theoretical, numerical and experimental studies are needed to clarify and resolve this controversial issue.

Figure 5 that the relaxation of the AC susceptibility on our time scale is as large as in real experiments, the relaxing signal being bigger for χ'' than for χ'. This explains why the study of χ'' is usually preferred in laboratory experiments. For χ'' the amount of relaxation is nearly equal to the corresponding stationary ($\omega t \rightarrow \infty$) value.

5 Conclusions

In this paper we have made a detailed study of the dynamical scaling behavior of the correlation functions and AC susceptibilities in the aging regime for spin glasses. The study has been done applying the scaling behaviors preferred by the experimentalists and comparing them with the results obtained in numerical simulations of the three dimensional Edwards-Anderson model.

The general conclusion is that there is a full agreement between the experimental results measured for TRM decays and simulations for correlations. This agreement must be understood in the following sense. All data collected for spin glasses is well compatible with a full aging scaling scenario, probably with logarithmic corrections, although these subdominant corrections are difficult to be detected experimentally.

It is also interesting to see how the parameters obtained in the fits of the decay of the correlation function agree with the equivalent parameters for the TRM in experiments, suggesting a universality in the dynamical scaling of relaxations which is well captured by the Edwards-

References

1. L. Lundgren, P. Svedlindh, P. Nordblad, O. Beckman, Phys. Rev. Lett. **51**, 911 (1983).
2. J. Hammann, M. Ocio, E. Vincent, in *Relaxation of Complex Systems and Related Topics*, edited by I. Campbell, C. Giovanella (Plenum Press, New York, 1990).
3. E. Vincent, J. Hamman, M. Ocio, J.P. Bouchaud, L.F. Cugliandolo, in *Complex behavior in glassy systems*, *Proceedings of the XIV Sitges Conference 1996*, edited by M. Rubí, C. Perez-Vicente (Springer-Verlag, 1997).
4. P. Nordblad, P. Svedlindh, in *Spin Glasses and Random Fields*, *Series on Directions in Condensed Matter Physics*, Vol. 12, edited by A.P. Young (World Scientific, 1998).
5. J. Hammann, E. Vincent, V. Dupuis, M. Alba, M. Ocio, J.P. Bouchaud, `cond-mat/9911269`.
6. H. Rieger, J. Phys. A **26**, L615 (1993); J. Phys. I France **4**, 883 (1994); Physica A **224**, 267 (1996).
7. J.O. Andersson, J. Mattsson, P. Svedlindh, Phys. Rev. B **46**, 8297 (1992).
8. J. Kisker, L. Santen, M. Schreckenberg, H. Rieger, Phys. Rev. B **53**, 6418 (1996).

9. T. Komori, H. Yoshino, H. Takayama, J. Phys. Soc. Jpn **68**, 3387 (1999); J. Phys. Soc. Jpn **69**, 1192 (2000).

10. S.F. Edwards, P.W. Anderson, J. Phys. F **5**, 965 (1975).

11. The most recent evidence for a finite-temperature phase transition in 3D spin glasses is for the $\pm J$ model: N. Kawashima, A.P. Young, Phys. Rev. B **53**, R484 (1996); M. Palassini, S. Caracciolo, Phys. Rev. Lett. **82**, 5128 (1999); A. Hartmann, Phys. Rev. E **59**, 84 (1999); H.G. Ballesteros *et al.*, Phys. Rev. B **62**, 14237 (2000).

12. E. Marinari, G. Parisi, J.J. Ruiz-Lorenzo in *Spin Glasses and Random Fields*, *Series on Directions in Condensed Matter Physics*, Vol. 12, edited by A.P. Young (World Scientific, 1998).

13. C. Battista *et al.*, Int. J. High Speed Comp. **5**, 637 (1993).

14. L.F. Cugliandolo, J. Kurchan, F. Ritort, Phys. Rev. B **49**, 6331 (1994).

15. G. Parisi, F. Ricci-Tersenghi, J.J. Ruiz-Lorenzo, Eur. Phys. J. B **11**, 317 (1999).

16. S. Franz, H. Rieger, J. Stat. Phys. **79**, 749 (1995).

17. E. Marinari, G. Parisi, F. Ricci-Tersenghi, J.J. Ruiz-Lorenzo, J. Phys. A **31**, 2611 (1998).

18. H. Rieger, Ann. Rev. Comp. Phys. **2**, 295 (1995).

19. For multiscaling effects in the aging dynamics of the O(n) model see L. Berthier, Eur. Phys. J. B **17**, 689 (2000). Other simple models which have been shown to display logarithmic corrections are the oscillator model with Monte Carlo dynamics, L.L. Bonilla, F.G. Padilla, F. Ritort, Physica A **250**, 315 (1998); and the Backgammon model, C. Godreche, J.M. Luck, J. Phys. A **30**, 6245 (1997).

20. E. Vincent (private communication).

21. L.W. Bernardi, H. Yoshino, K. Hukushima, H. Takayama, A. Tobo, A. Ito, Phys. Rev. Lett. **86**, 720 (2001).

22. E. Marinari, G. Parisi, F. Ricci-Tersenghi, J.J. Ruiz-Lorenzo, J. Phys. A **33**, 2373 (2000).

23. T. Komori, Yoshino, H. Takayama, J. Phys. Soc. Jpn **69**, 228 (2000).

24. M. Picco, F. Ricci-Tersenghi, F. Ritort, Phys. Rev. B **63**, 174412 (2001), `cond-mat/0005541`.

25. H. Yoshino, A. Lemaitre, J. P. Bouchaud, Eur. Phys. J. B **20**, 367 (2001) `cond-mat/0009152`.